BACHELOR THESIS

Concept origami-based, magnetic, surgical capsule robot for the purpose of aneurysm coiling

THIJS BROKERS

FACULTY OF ENGINEERING TECHNOLOGY
DEPARTMENT OF BIOMECHANICAL ENGINEERING

EXAMINATION COMMITTEE
PROF.DR. S. MISRA
DR. V. KALPATHY VENKITESWARAN
DR. A. SADEGHI

JULY 12TH, 2024

UNIVERSITY OF TWENTE.

Thesis submitted by
Thijs Brokers
under the supervision of
Dr. V. Kalpathy Venkiteswaran,
Prof.Dr. S. Misra, and
Dr. A. Sadeghi
in order to fulfill the necessary requirements to obtain a Bachelor's degree in
Biomechanical Engineering at the University of Twente
and defended on
Thursday, 12th of september, 2024

Acknowledgement

During the time that I worked on my bachelor thesis, I was provided with excellent support from multiple parties. Therefore, I would like to thank the following people:

First of all, I would like to thank my daily supervisor dr. V. Kalpathy Venkiteswaran for guiding me through my first time doing independent research within a research group. His advice and guidance helped me to get the most out of my bachelor thesis. Especially his help during the 3D modelling was invaluable, as I had never done this before.

Secondly, I would like to thank Prof.Dr. S. Misra and Dr. A. Sadeghi for taking the time to evaluate my thesis. I do not doubt that their feedback will be of great help in the writing of my master thesis later on.

Lastly, I would like to thank my family and girlfriend for always being there for me during the more difficult times of my thesis period. They have always been supportive and understanding when I needed it most.

Thijs Brokers
July 12, 2024

Abstract

In this paper a concept origami-based, magnetic, surgical capsule robot for the purpose of aneurysm coiling is proposed. The design is intended to be an alternative to simple coiling, which is a minimally invasive procedure to treat aneurysms by filling them with platinum coils via a catheter. Unlike simple coiling, the origami-based magnetic capsule closes the aneurysm with a single rigid structure. Furthermore, the capsule is transported and deployed using magnetic actuation, eliminating the need for catheters. This subsequently ensures better closure of the aneurysm and a less invasive treatment. After a full analysis of the design, it is concluded that the capsule can only be used to treat aneurysms with sizes of approximately 5 mm or smaller. Aneurysms at these sizes have a low chance of rupture, causing the capsule to be more appropriate as a preventive treatment. In this way, smaller aneurysms can be treated before they become a threat to the patient's health. In addition, it was examined whether the required magnetic field strength and gradient for the magnetic actuation had attainable/ realistic values. This turned out not to be the case, but with several suggested adjustments these values could be brought to suitable levels. To show that it is possible to have a capsule unfold magnetically, a paper prototype was tested. The result of the prototype confirms that the described unfolding technique can indeed be used.

Dutch version:

In dit artikel wordt een concept voor een origami, magnetische, chirurgische capsule robot ten behoeve van aneurysma dichting voorgesteld. Het design zou een alternatief moeten bieden voor simple coiling, wat een minimaal invasieve behandeling is waarin een aneurysma wordt gevuld met platina draden via een katheter. In tegenstelling tot simple coiling vult de op origami gebaseerde magnetische capsule het aneurysma met één enkele rigide structuur. Verder, wordt de capsule getransporteerd en ingezet met magnetische besturing, waardoor er geen katheters meer nodig zijn. Dit zorgt er opeenvolgend voor dat het aneurysma beter wordt gedicht en dat de behandeling minder invasief is. Na een volledige analyse van het design wordt er geconcludeerd, dat de capsule alleen kan worden gebruikt om aneurysma te behandelen, die ongeveer 5 mm of smaller zijn. Aneurysma van deze grote hebben een kleine kans op scheuren, waardoor de capsule beter kan worden toegepast als een preventief behandeling. Op deze manier kunnen kleinere aneurysma worden behandeld, voordat ze een gevaar vormen voor de patiënts gezondheid. Hiernaast is er ook gekeken of de magnetische veld sterkte en gradiënt verkrijgbare/ realistische waardes hebben. Dit lijkt niet het geval te zijn, maar meerdere aanpassingen zijn voorgesteld, die de waardes naar een meer geschikt niveau zouden kunnen brengen. Om te laten zien dat het mogelijk is om de capsule magnetisch te laten ontvouwen, is er een papieren prototype getest. Het resultaat van het prototype bevestigd, dat de magnetische ontvouw techniek daadwerkelijk kan worden toegepast in het design.

Table of Contents

List of Figures

List of Tables

1 Problem Analysis

1.1 Saccular aneurysms

Brain aneurysms occur at weak spots in the blood vessel walls of the brain, which expand under pressure and fill with blood. These types of aneurysms, most commonly called Intracranial Aneurysms (IAs), are found in approximately 2%-5% of the population [2,3]. Saccular (or Berry) aneurysms, which are blood sac formations on the side of an artery (see Figure 1), are the most common type of cerebral aneurysm. This type of aneurysm could go unnoticed, but in the worst case, it causes a rupture of the involved blood vessel. In the latter case, the patient gets a hemorrhagic stroke. A subtype of this is subarachnoid hemorrhage (SAH), which involves blood flowing into the subarachnoid space (area between brain and skull) where it can damage brain tissue, like the blood-brain barrier. Around 85% of cases with aneurysmal SAH arise from a saccular aneurysm [4]. Therefore, preemptive treatment of saccular aneurysms may lead to a decrease in aneurysmal complications, like hemorrhagic strokes.

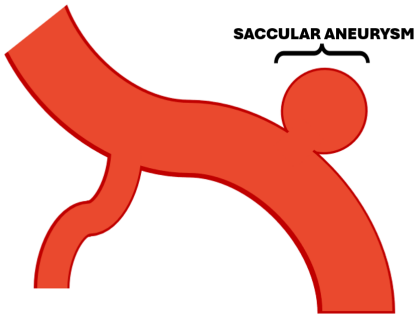

Figure 1: Schematic overview of a saccular aneurysm. The aneurysm is formed by stretching of the artery wall at a weak point.

1.2 Aneurysm treatment

There are multiple techniques available for treating IAs, each having its own advantages. Based on the nature of the aneurysm, one has to decide which technique should be used. Saccular aneurysms can be treated with surgical clipping, cerebral bypass, stenting, and simple coiling [5].

Surgical clipping requires a section of the skull to be removed, through a process called craniotomy, to gain access to the aneurysm site. After this, the sac of the aneurysm is clipped off from the rest of the blood circulation, which prohibits the aneurysm from growing any further. Cerebral bypass also requires a craniotomy, but instead of blocking off the aneurysm, the blood circulation is changed so that the blood bypasses the aneurysm and the associated arteries. This is achieved by reconnecting blood vessels in and/or around the brain [5]. In the case of stenting and coiling, there is no need for cranial incisions. Instead, these techniques require the materials to be inserted near the groin region and directed to the aneurysm through the body's blood vessels. A stent is a small cylinder, which can be expended within the blood vessel to which the aneurysm is attached. Within the vessel, it reinforces the walls or diverts blood flow away from the aneurysm. Coiling, on the other hand, directly fills the aneurysm to reduce blood inflow. To achieve this small platinum wires are inserted into the aneurysm to fill it. This is often followed by blood coagulation and the formation of granulation tissue around the wires, which further closes the aneurysm. This only works for saccular aneurysms with dome-to-neck ratios ≥ 1.6, see Figure 2. If this is not the case the aneurysm entrance is too large compared to its volume and the coil can be flushed out. Therefore, smaller dome-to-neck ratios often require adjunctive techniques like stents to keep the coil in its place [5–7]. Based on this, aneurysm coiling is a good option for minimum invasive and minimal risk saccular aneurysm treatment, if

the dome-to-neck ratio is favourable [5,8]. It does however still have some drawbacks. Recurrence caused by coil compaction, coil migration, and incomplete filling of the aneurysm can occur, making that around 12% of all coil treatments require a follow-up [9]. An improvement or variation on this technique could reduce the number of secondary operations.

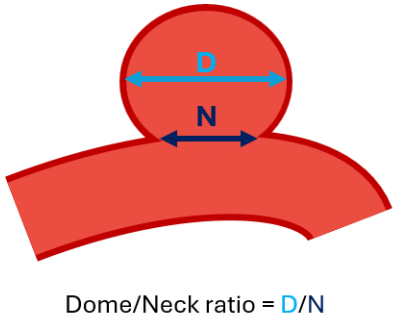

Figure 2: Definition of the dome-to-neck ratio in aneurysms.

1.3 Magnetic origami capsule

Instead of coiling the aneurysm with platinum wires, it might be more sufficient to fill it with a single firm structure. This fixes some of the mentioned problems of platinum coiling, that could lead to resurgence of the aneurysm. However, the width of the aneurysm sac is larger than the width of its neck or even the blood vessel. For a single object to fit through the aneurysm's neck and still fill the entire volume, it needs to be compressed and released within the sac. A foldable origami structure might fulfil this task. Origami structures have already been studied for the purpose of aneurysmal stenting, such as in the study by Kuribayashi et al., where an origami stent graft was fabricated with TiNi shape memory alloy foil [10]. Now, the challenge arises to use similar techniques to create a spherical filling for the aneurysm, which can be folded into a more compact capsule-like shape. This compact shape allows the capsule to fit through the blood vessels. The width of the capsule is, however, still much larger than the thin platinum wires, that are normally administered via catheters. The usage of catheters might therefore not be possible and other administration methods must be considered.

In this report a concept origami capsule, for the purpose of aneurysm filling is proposed. Instead of a catheter the capsule will be actuated and deployed, with the usage of magnetic actuation. Magnetic actuation of small origami structures has already been achieved, such as in the research of Ze et al., in which they created spinning-enabled wireless amphibious origami millirobots, which could move through a pig stomach filled with viscous fluid. The millirobots are based on the kresling origami pattern and are a great example of magnetic field guided actuation [11]. Similar techniques will be employed to create an up-scaled prototype aneurysm-filling origami capsule, which will be evaluated on its ability to be magnetically actuated and its potential in aneurysm treatment.

2 Background

2.1 Magnetically actuated origami soft robots

Magnetically actuated origami soft robots are widely studied in biomedical research. They can be used for everything from drug delivery to performing minimally invasive surgeries within the human body. What these origami robots have in common is the fact that they are controlled with magnetic fields and gradients. This is achieved by incorporating magnetic material within/ on their origami panels, which allows controlled actuation of the origami shape [12, 13]. In the article by Xu et al., multiple kinds of flexible robot motions are displayed. A few of these types of motion are: gripping, swimming, jumping, and crawling [13]. These examples show the versatility of magnetic origami robots. For this reason, we will look into the possibility of using this type of soft robot to navigate to and fill an aneurysm within the brain.

2.2 Capsule dimensions

Around 85% of saccular aneurysms originate from the arteries of the circle of Willis. The most common places where they are found are the anterior communicating artery, the internal carotid artery, the middle cerebral artery, and to a lesser extent the posterior circulation sites, like the basilar artery tip [14, 15]. The diameter of these arteries can vary within a range of approximately 0.5 to 5 mm, with some deviation [16]. Therefore, it is necessary that the folded origami structure can pass through vessels with these dimensions. At this size, the origami structure must still be capable of filling aneurysms, with dome widths varying from millimetres to a few centimetres [17]. This highlights the importance of the unfolded-to-folded diameter ratio (R), as shown in Figure 3. The size limitations do not apply to the up-scaled prototype, but the diameter ratio should be scalable.

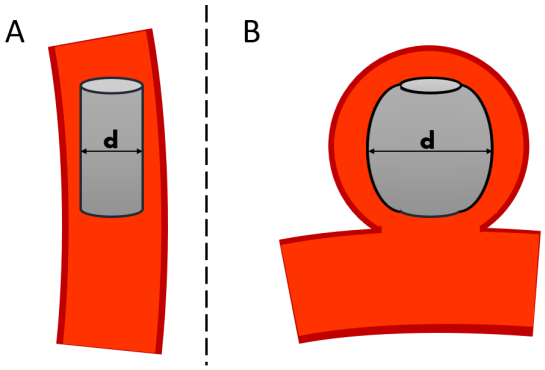

Figure 3: Visualisation of the diameter change after the capsule unfolds itself to fill an aneurysm. A) Capsule diameter in the folded state, and B) Capsule diameter in the unfolded state.

2.3 Magnetic actuation of origami capsules

Actuation of soft robots by the usage of external magnetic fields is a promising new technique in the field of bio-robotics. The promise of this technique is that it enables wireless control of robotic movement, which makes it excellent for accurate actuation of robots that function within the human body [18]. These robots have actuators covered and/ or inserted with permanent magnets, that try to align their magnetic dipole moment with the external field. This alignment takes place, because of the magnetic forces and torques that are applied on the magnets by the external field.

In an uniform magnetic field a magnet (m) has a misaligned magnetic moment, as shown in Figure 4. A torque (τ) is generated that rotates the magnet to align its poles with the magnetic field. This torque can be calculated with Formula 1 [19].

$$\tau = B \times m \tag{1}$$

where:

τ is the torque on the magnet $[N \cdot m]$
B is the external magnetic vector field $[T]$
m is the magnetic dipole moment $[A \cdot m^2]$

As can be seen in Formula 1, the strength of the magnetic field (B) and the magnet's dipole moment (m) both influence the amount of torque being generated. What's more, the effect of alignment is also seen in the formula due to the use of the vector product. The magnitude of this vector product can be described using Formula 2.

$$|\tau| = |B||m| \sin\theta \tag{2}$$

where:

$|\tau|$ is the magnitude of torque on the magnet $[N \cdot m]$
$|B|$ is the magnitude of the external magnetic field $[T]$
$|m|$ is the magnitude of the dipole moment $[A \cdot m^2]$
θ is the angle between the two vectors [radians]

When the angle between the magnetic dipole moment and the external magnetic vector field is 0, they are aligned. As expected this results in zero torque being generated, as the sinus term also becomes 0. With the same formula, we can determine the angle that causes the highest amount of torque, which is $\frac{1}{2}\pi$. Therefore, the strongest torque is present as the magnetic dipole moment and external magnetic field are perpendicular to each other. By changing the direction and magnitude of the external magnetic field it is possible to precisely generate a magnetic torque if the magnet's current orientation is known.

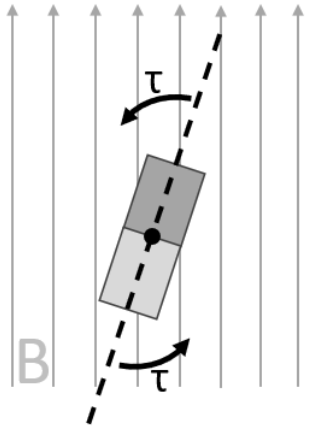

Figure 4: The torque applied on a magnet to align its magnetic dipole moment with the external magnetic field.

In the case that the external magnetic field is nonuniform, a magnetic force is generated. The force exerted on a magnet can be calculated using Formula 3. If the magnet is misaligned in the nonuniform field, both the magnetic force and magnetic torque will work on the magnet [19]. A visualisation of the magnetic force on a dipole moment in a nonuniform magnetic field is shown in Figure 5. The dipole moment has an orientation opposite to the direction of force, as it is aligned with the magnetic field direction.

$$F = (m \cdot \nabla)B \tag{3}$$

where:

F is the amount of force exerted $[N]$

∇ is the gradient operator
B is the strength of the external magnetic field $[T]$
m is the magnetic dipole moment $[A \cdot m^2]$

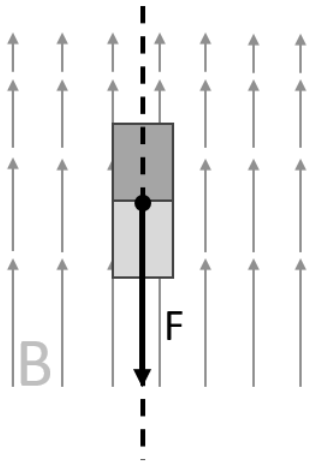

Figure 5: The magnetic force applied on magnetic dipole moment in a nonuniform magnetic field. The magnetic dipole moment is in the opposite direction of the force.

We make use of the principles of magnetic torque and force to guide and unfold the origami capsule within the human body. The magnitude of these forces can be varied by adjusting the strength of magnetic dipoles on the capsule and by varying the strength of the magnetic field. The magnetic dipole moments cannot be changed once implemented in the capsule, which means that a change in magnetic actuation can only be caused by adjusting the external magnetic field. We can use the magnetic field to change the configuration of the origami panels with an associated magnetic dipole or to move the entire capsule. This leads to a wide variety of possible motions, such as crawling, walking, swimming, and dragging [12, 20]. Besides these types of motion, unfolding the capsule can also be achieved by changing the orientation of the origami panels. Magnetic actuation makes it possible to guide the capsule to the aneurysm site and unfold it within the aneurysm dome.

2.4 Shape-Memory Polymers

As previously stated magnetic actuation can be used to unfold the origami capsule. However, more complicated origami structures require a wider range of magnetic dipole-moment orientations, which would make the fabrication process difficult. In this case, a Shape-Memory Polymer (SMP) would be an alternative. SMP's are a type of material that can retain a shape after being exposed to external or physiological stimuli. At the polymers transition temperature, the polymer chains are kept organised by cross-linking bonds. If the temperature is decreased it is possible to deform the capsule to the desired shape, because the polymer chains are no longer able to move freely. If we increase the temperature of the polymer past its transition temperature, the chains can again move freely and the cross-links cause the object to regain its initial shape. If the origami capsule is made out of an SMP and produced in the shape of the unfolded state, it is possible to retain its shape after heating the SMP beyond its transition temperature. Inductive heating of the SMP can be achieved by creating an alternating magnetic field with the setup that is already present for magnetic actuation [21]. This makes SMPs a very good alternative for switching between folding states. It might also be possible to combine the technique with magnetic actuation, to increase the unfolding efficiency.

3 Requirements and constraints

The eventual concepts are graded based on their ability to perform the task at hand. Requirements and constraints have been established to make the required properties measurable. A description of the requirements and constraints follows:

1) Magnetic transportation In order to actuate the permanent magnet(s) present in the capsule, a magnetic field needs to be applied. Depending on the position, orientation, and direction of movement of the magnet(s) the appropriate magnetic field needs to be generated. The complexity of this magnetic field increases when multiple magnets need to move in different directions within the same workspace. Therefore, the angles between the field's directional vectors must have low variation to keep the complexity of the field manageable within the workspace.
2) Capsule flexibility The blood vessels of the human body have complex layouts and bend in different directions. These bends make it more difficult for elongated structures, such as the capsule, to move unhindered through the vascular system. A more flexible capsule is preferred because it bends to the shape of the vessel and reduces the risk of damage to the blood vessel walls. Here flexibility is defined as the angle that the front can make relative to the midline of the capsule.
3) Ease of production The amount of folds present in the origami capsule directly influences the difficulty of production. More complex origami structures have more folds and therefore a greater chance of failure. Misalignment of panels, for example, causes the structure to fold incorrectly or prevent folding completely. Therefore, origami structures with fewer folds are preferred.
4) Unfolded-to-folded diameter ratio (R) As previously mentioned in Section 2.2, an aneurysm has most often larger dimensions than the blood vessel through which the capsule passes. This makes it necessary for the capsule to increase its diameter after locating itself in the aneurysm. Origami structures with high folded-to-unfolded diameter ratios can pass through small vessels while being able to fill aneurysms with far larger dimensions. This highlights the importance of the diameter ratio.
5) Strength in fold direction Blood will still try to flow into the aneurysm even after the capsule is situated in the aneurysm. This flow causes a compressive force along the vertical axis of the capsule. This compressive force must not work in the folding direction, as it would cause the origami structure to fold back into its compressed state. This would dramatically decrease the effectiveness of the capsule.
6) Shape unfolded state Saccular aneurysms are generally spherical shaped [22]. By closely mimicking the aneurysm shape while being unfolded, the origami capsule is firmly secured in its place and restricts the entire inner volume from blood flow. By comparing the capsule's volume to that of a sphere with a similar width, we can determine how closely the structure matches the spherical shape of the aneurysm. This is under the assumption that the width-to-height ratio in the unfolded state is $0.9 \leq R \leq 1.1$, so adjusting the height cannot result in a more favourable volume ratio.

4 concepts have been graded based on the requirements & constraints mentioned in the previous section. These concepts are found in Appendix A.1 - A.4 and their evaluation can be found in Appendix A.6. The evaluation is done on a 1-5 scale for every requirement & constraint. Based on its importance an extra weight factor is added (1-3), which ensures that the most important functionalities are present in the highest-graded concept. The grading criteria can be found in Appendix A.5. The concept that best met the requirements & constraints is design B and will therefore be developed further.

4 Concept

4.1 Concept description

Design B is a cuboid-shaped capsule, that can be unfolded to have a more sphere-like shape. This is achieved by adding inwards folded triangles between the rectangular-shaped sides, which when unfolded give the shape change described in Figure 6. This means that the capsule has two states in which it can operate. These states are the folded state and the unfolded state. In the folded state the capsule has a diameter small enough to let it fit through the blood vessels when travelling to the aneurysm site. In this state, the capsule is dragged through the blood vessels by an applied magnetic force. As described in Section 2.3, the application of a magnetic force requires the capsule to have a magnetic dipole moment in the opposite direction of motion. This magnetic dipole moment is not only used to drag the capsule, but also to orientate it within the vessels by applying a magnetic torque. The orientation and magnitude of this dipole moment is therefore important for the capsule's movement in this state.

The unfolded state is deployed when the capsule has arrived on site. The shape change is initiated by rotating the rectangular sides outward, as described in Figure 6. These rotations require torques to be placed on each individual side and only works if the sides behave as rigid objects. Therefore, the sides are made out of a rigid material and connected to each other with a more elastic material to allow folding. On the rigid panels magnetic dipole moments are placed to allow them to be rotated by magnetic torque. The capsule becomes completely unfolded when the applied magnetic field generates the magnetic torques necessary to overcome the resistance of the elastic material to deformation. Once unfolded, the blood pressure compresses the capsule in the vertical direction. This force locks the shape of the capsule, as it resists further outward deformation. If the proportions of the capsule are chosen correctly the capsule should completely block blood flow to the aneurysm.

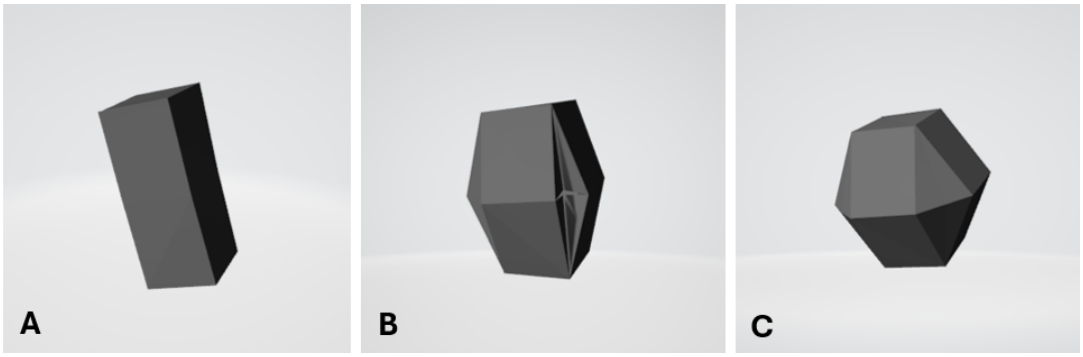

Figure 6: Capsule shape at different unfolding stages: A) folded, B) intermediate state, and C) unfolded.

4.2 Magnetic dipole moments

As previously stated the origami capsule is completely controlled by magnetic actuation. This requires the placement of multiple magnetic dipole moments that: A) Make magnetic transportation of the origami capsule through the human body possible, and B) Unfold the capsule once it arrives at the desired location. The transportation of the magnetic capsule is achieved by a combination of magnetic force and torque, as discussed in the previous section. For this purpose two magnetic dipole moments are added orthogonal to the capsule's bottom and top, which act together as one larger dipole moment. This dipole moment defines the direction of motion, as the capsule is pulled through a magnetic gradient in the opposite direction of its dipole moment. The dipole moments responsible for unfolding the capsule are placed orthogonal to the capsule's sides to ensure maximum magnetic torque, as discussed in Section 2.3. The orientation of these dipole moments determines the rotational direction of the sides. Arranging the dipole moments as shown in Figure 7, gives the orientations necessary to unfold the capsule. The magnetic field used in this step needs to be homogeneous to ensure that only magnetic torque is generated. This would otherwise result in a magnetic

force being applied when the capsule is in the aneurysm. The following displacement could potentially damage the inside of the aneurysm. Another thing to be wary of is that the magnetic gradient, needed for transportation, should not have local magnetic values strong enough to unfold the capsule. Otherwise, the capsule unfolds before it reaches the treatment site.

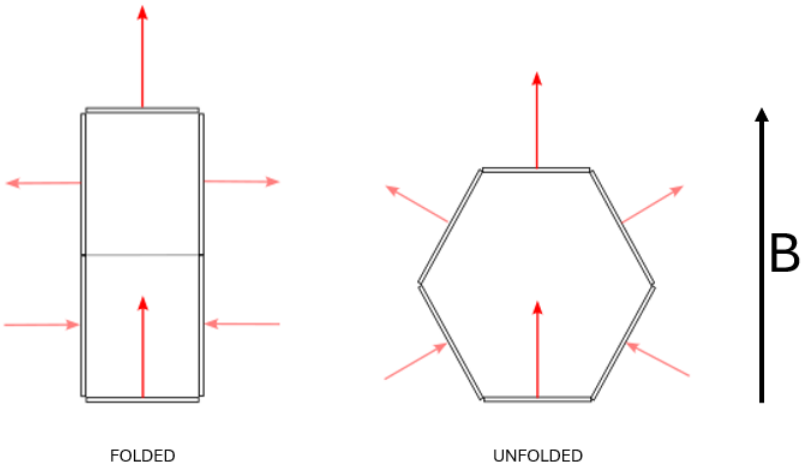

Figure 7: Magnetic dipole moments of the origami capsule plates. The dipole moments on the top and bottom are used to guide the capsule through the human body by an acting magnetic force. The dipole moments on the sides unfold the capsule by an acting magnetic torque. The directions of the dipole moments on the sides are chosen to have an angle of 90 degrees with the external magnetic field to ensure maximal magnetic torque. The dipole moment orientations are the same for each side-view.

4.3 Material choice

The rigid material chosen for the origami plates is the polymer polylactide (PLA). PLA is a biocompatible thermoplastic, that can be used in combination with 3D printing techniques. It biodegrades in the human body to lactic acid or carbon dioxide and water. The material is widely used as biomaterial [23]. Because of PLA's biocompatibility, the body can be safely exposed to it for a prolonged time. It does, however, biodegrade which means that it will lose its strength over time when exposed to bodily fluids. Therefore, it requires a coating with a bio-inert material.

The PLA plates are going to be placed in a silicone frame. Silicone is a material well known for its flexibility, inertness, and biocompatibility. Furthermore, silicone is also used as a coating to increase the biocompatibility of medical devices [24]. The silicone frame provides the flexibility needed to create folds between the PLA plates and forms a coating that protects the PLA from being biodegraded. Due to the inertness of silicone it is not possible to directly connect the silicone to the PLA plates. This is however, not needed as the plates are completely enveloped within the silicone frame. For this design, the silicone PDMS is chosen.

The magnitude of the magnetic dipole moments used is dependant on the type of magnetic material. Ideally, a strong magnetic material is used to keep the required magnetic field value and gradient to a minimum. Therefore, neodymium n52 magnets are implemented, as neodymium magnets are the strongest commercially available permanent magnets [25]. It should be noted however, that neodymium magnets have poor biocompatibility and should therefore not be directly exposed to the human body [26]. Therefore, the magnets must be implemented within the silicone structure to improve biocompatibility.

5 Concept analysis

5.1 Treating different sized aneurysms

As previously stated aneurysm sizes vary from a few millimetres to a few centimetres [17]. If we want to treat this wide range of aneurysm sizes, the origami capsule needs to be made with different R-values. In Figure 8 it is seen that the width of the unfolded capsule (U_{width}) is dependent on the length of the side panels (S_{length}) and the width of the triangular connection (T_{width}). There are, however, limitations to these sizes and therefore the achievable R-values.

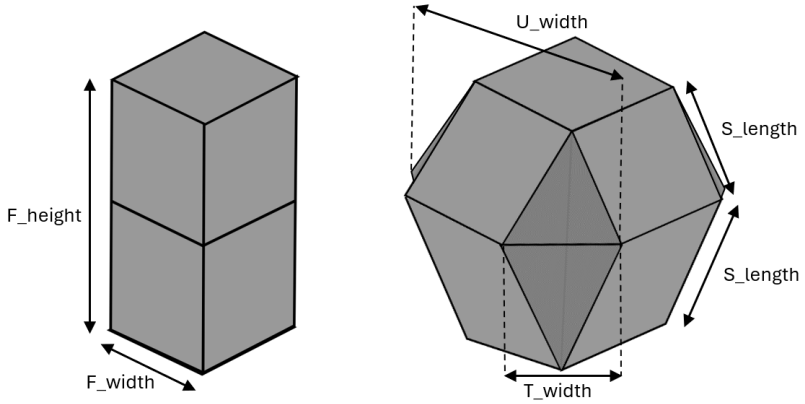

Figure 8: Reference dimensions of the folded (left) and unfolded (right) origami capsule.

5.1.1 Unfolded capsule shape

The first limitation that we consider is the shape of the unfolded capsule. The unfolded capsule shape must closely resemble the shape of the spherical berry aneurysm. This ensures proper fixation of the capsule within the aneurysm dome. For this reason, the side length and triangular width are chosen, so the resulting unfolded capsule has equal width and height similar to a sphere. Due to the set relationship between these two parameters, it is now possible to relate the desired R-value to the height-to-width ratio of the folded capsule (see Figure 9). An object can, however, have an equal width and height without it being spherically shaped. For this reason, the sphericity is calculated for the unfolded capsule shapes of different R-values. The sphericity is a value that tells how closely an object's shape resembles that of a sphere. Spheres for example have a sphericity of 1.0, while cubes have a sphericity of 0.81 [27,28]. The formula for sphericity is shown in Equation 4.

$$sphericity = \frac{\pi^{1/3} * (6V_o)^{2/3}}{A_o} \tag{4}$$

where:
V_o is the objects volume $[m^3]$
A_o is the objects surface area $[m^2]$

As can be seen in Figure 10, the sphericity of the unfolded capsule peaks at an R-value of circa 2.6, after which it starts to decline. The desired sphericity is chosen to be equal to or larger than that of a dodecahedron ($\geq$ 0.91) [28]. Therefore, capsules with an R-value of 1.8 - 6 are deemed to have the right shape to fill spherical-shaped aneurysms. This assumes, however, that there is no limitation placed on the sizes of S_{length} and T_{width}. The triangular plates, for example, must fit into the folded capsule. This is only possible if

they do not extend past the centre line of the capsule. This is only the case for R-values ≤ 3.1. This alone decreases the usable R-value range to 1.8 - 3.1.

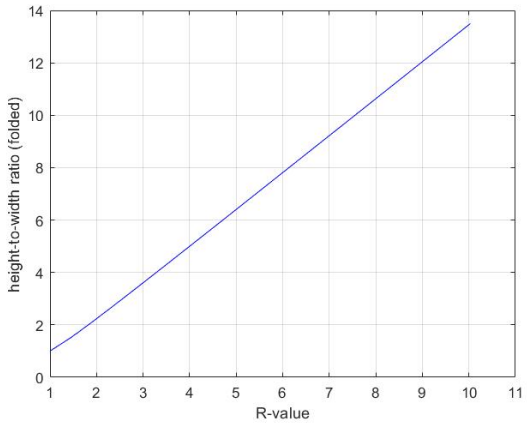

Figure 9: Relationship between the unfolded-to-folded diameter ratio (R) and the height-to-width ratio in the folded state.

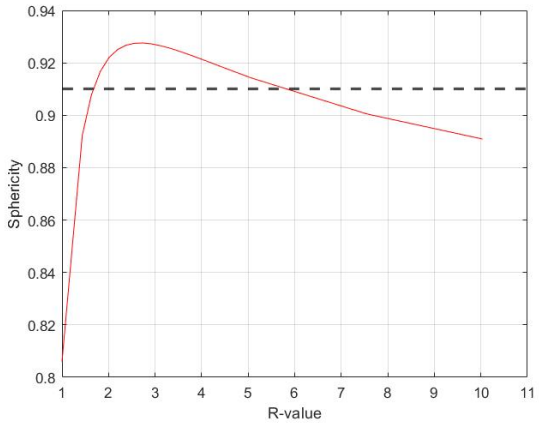

Figure 10: Sphericity as a function of the unfolded-to-folded diameter Ratio. A line has been drawn at a sphericity of 0.91.

5.1.2 Folded capsule size

The second limitation that we consider is that of the folded capsule size. While travelling through the blood vessels the capsule must not block blood flow or get stuck at vascular bends. For peripherally inserted central catheters a catheter to vein ratio (CVR) of < 0.45 is considered to limit the effect of thrombosis [29]. Unlike a catheter, the capsule does not block blood flow along the entirety of the traversed blood vessels. Therefore, it is assumed that we can use this value to estimate the percentage of cross-sectional area that is allowed to be blocked by the capsule. This value is 20 % of the total cross-sectional area. With this information, we can calculate the maximal width of the capsule to be 0.4 times the width of the blood vessel.

With the width of the capsule known it is possible to calculate the maximum capsule length to traverse vascular bends of different angles. In Figure 11 a visualisation is shown of the proportions at which the capsule can no longer pass through a bend of β degrees.

With the geometry shown in Figure 11 it is possible to draw up the formula for the maximum capsule length, shown in Equation 5. Because the blood vessel is cylindrical shaped the distance between the capsule and vessel walls decreases as we move further away from the midsection. Therefore, we use blood vessel width at the cross section that has the least distance between the capsule and vessel wall. At this point the width is equal to 0.92 vessel diameter.

$$l_{max} = 2\cot(\frac{1}{2}\beta)(0.92b - w \cdot \cos(\frac{1}{2}\beta)) \tag{5}$$

where:

β is the bending angle [radians]
b the blood vessel diameter $[m]$
w is the folded capsule width $[m]$

If we make use of the fact that b is equal to $2.5w$ we find the relationship between folded capsule width and maximum capsule length at different β-values, as shown in Figure 12. It can be seen that increasing the bending angle greatly reduces the capsule length that can be used. Furthermore, the ramps in this plot

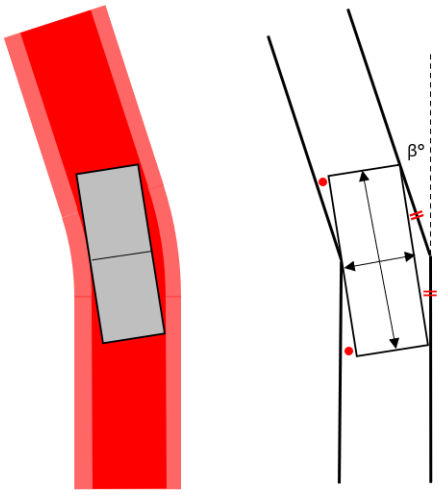

Figure 11: Maximal capsule proportions after which traversal through the vascular bend is no longer possible.

are equal to the maximum height-to-width ratio, that a capsule can have at that bending angle. Using the relationship between the folded height-to-width ratio and the R-value, shown in Figure 9, we find the R-values that are achievable when dealing with different bending angles. These R-values are plotted in Figure 13. In the Figure it can be seen that the maximum R-value is reduced to 2.3 if the capsule needs to travel passed a 90 degree bend. This would further restrict the previously mentioned range of usable R-values. Therefore, the aneurysm location and capsule path determine the maximum aneurysm size that can be treated using this technique.

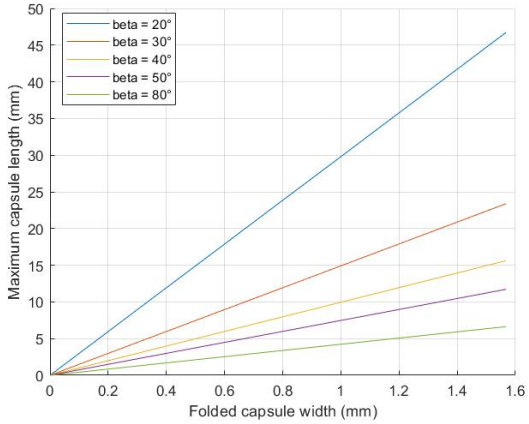

Figure 12: Relationship between the maximum capsule length and blood vessel width at different β-values.

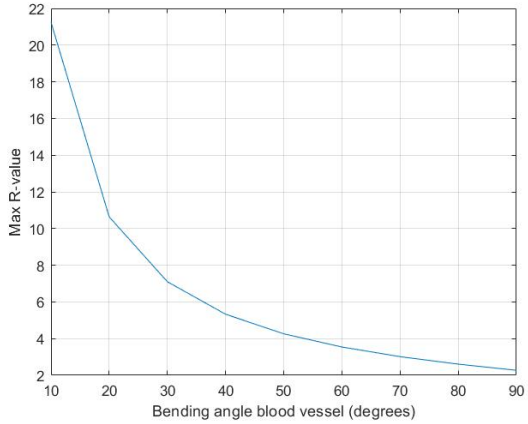

Figure 13: Relationship between bending angle and the capsules max R-value.

5.2 Fluid dynamics

To calculate the magnetic gradient necessary to pull the capsule through the bloodstream, we must know the forces acting on the capsule. These forces are gravity, buoyancy, and drag. If the magnetic gradient creates a magnetic force equal to and opposite to the net counteracting force, the capsule is able to move at a constant speed through the bloodstream.

We first consider the drag force experienced by the capsule. The multiphysics software COMSOL is used to simulate blood flow over a cuboid. The cuboid in question has a width of 0.4 mm and a height of 1 mm. It is simulated to be in a blood vessel, with a diameter of 1 mm and length of 5 mm. The ratio between the capsule width and blood vessel diameter is 0.4, which is in line with the requisite mentioned in Section 5.1.2. The used values for blood density and viscosity are 1060 kg/m^3 and 5.5 cP. Blood is a non-Newtonian fluid, which means that the viscosity changes with the shear rate. In the article by Nader et al. a normal range for blood viscosity was assumed to be between 3.5 and 5.5 cP [30]. The highest value of 5.5 cP has been used in the model, to guarantee that the calculated drag force estimation is not too low. The mean relative blood velocities considered in the model are those in the range of 0.003 m/s to 0.5 m/s. This range combines the ranges of blood velocities in the arteries (0.1 - 0.5 m/s) and the blood velocities in the veins (0.003 - 0.05 m/s) [31]. It should however, be noted that the modelled blood vessel diameter is smaller than those where the velocities are based off. Therefore, we use this velocity range to get an estimation for the magnitude of the drag force. Running the simulation with a relative blood velocity of 0.5 m/s gives the flow velocity profile shown in Figure 14. The profile shown is for the mid-section of the blood vessel, with the cuboid centred in the middle. The resulting drag force is calculated by integrating the stress in the direction of fluid motion over the capsule's surface. The values for the fluid drag at different relative blood velocities are shown in Figure 15.

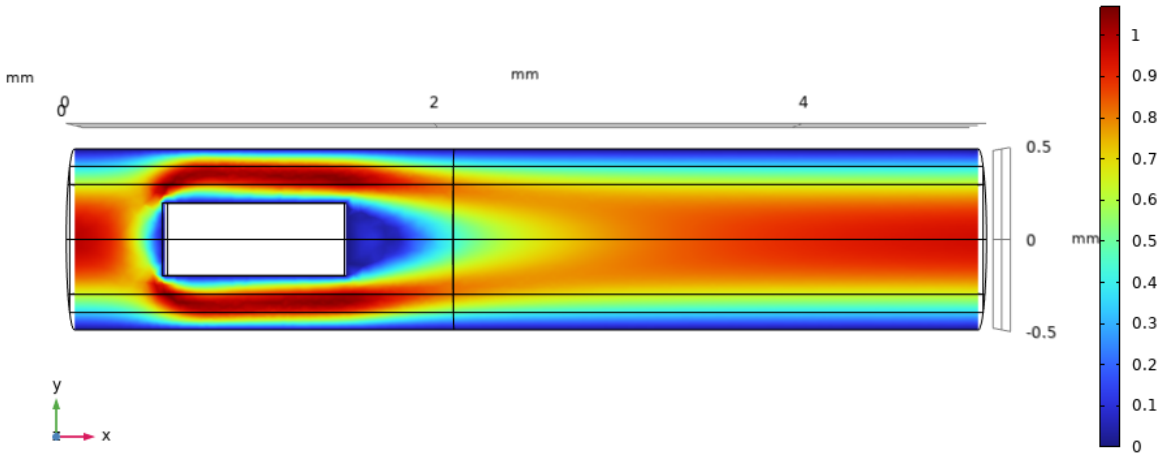

Figure 14: Fluid velocity profile at a mean relative blood velocity 0.5 m/s. The profile shown is that of the mid-section of the vessel, with the cuboid centred in the middle.

The next force that is considered is gravity. We simplify the geometry of the capsule to be that of a hollow cube. This cube has 4 panels of 0.4 by 1 mm and 2 panels of 0.4 by 0.4 mm. These panels have a thickness of 0.02 mm, which gives the hollow cube a volume of 3.84E-11 m^3. Each side has a 0.01 mm thick silicone and PLA layer. Therefore, we assume the density to be the average of the silicone PDMS (970 kg/m^3) and PLA (1240 kg/m^3) [32, 33]. This gives us the total gravitational force of 4.2E-7 N.

The last force we consider is buoyancy. As the capsule travels up from the insertion point it is pushed up by the displaced liquid. This force is called buoyancy and can be calculated by multiplying the volume of displaced liquid with the liquid density and the gravitational constant. Using the previously mentioned blood density of 1060 kg/m^3 and the known volume of the capsule, we can calculate the buoyancy to be 4.0E-7 N. Due to the similarity between the density of blood and the average density of the capsule, the gravitational force and the buoyancy are approximately the same. Therefore, we assume that they cancel each other.

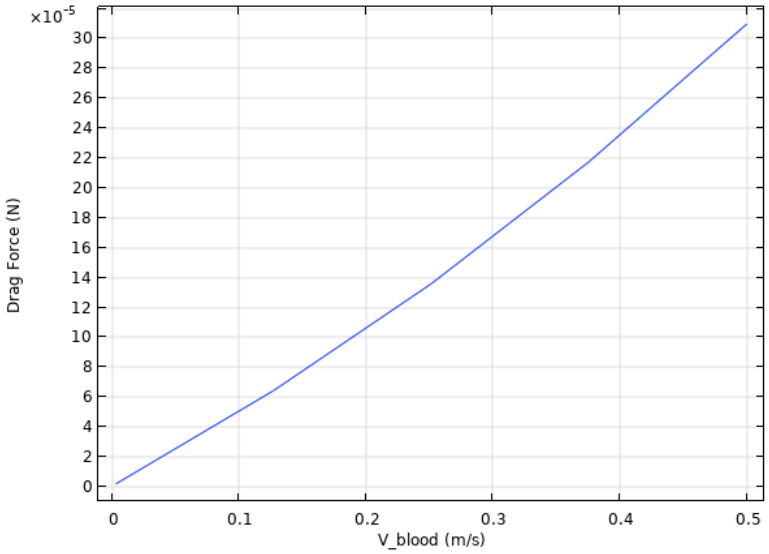

Figure 15: Fluid drag on the capsule at different relative blood flow velocities.

Based on this the magnetic force needs to be equal to the fluid drag for the capsule to move at a constant speed. According to Figure 15, the maximum amount of force caused by drag is 31E-5 N at a blood flow speed of 0.5 m/s. Using Formula 5, we can calculate the magnetic gradient needed to counteract the max amount of fluid drag. For this calculation, we need a value for the applied magnetic dipole moments along the vertical axis of the capsule, which are applied on the top and bottom plates. If we assume that these plates have neodymium n52 magnets with equal size attached to them, we can calculate the corresponding magnetic dipole moment. The two plates have a combined volume of 3.2E-12 m^3 and neodymium n52 has a residual flux density of 1.42 T [34]. With this information, we can calculate the magnetic dipole moment to be 3.61E-6 $A \cdot m^2$. Using these values in the formula for magnetic force, we can calculate the needed strength of the gradient to be 85.7 T/m. In the article by Li et al. a "Gradient-Enhanced Electromagnetic Actuation System" was made, that could achieve a maximum magnetic gradients of 20 T/m. This system was specifically made for microrobot manipulation [35]. The calculated maximum value for the magnetic gradient is 4.3 times larger than is achievable with this setup. It is, however, possible to decrease the needed magnetic gradient by increasing the magnetic volume or improving the capsule's fluid dynamics by changing the shape of the top.

5.3 Capsule folding

The multiphysics software COMSOL was used to approximate the magnetic field required to unfold the real-size capsule. The simulated capsule, shown in Figure 16, has a length of 1.04 mm and a width of 0.42 mm. 10 rigid panels of 0.014 mm thickness, are placed within the silicone frame with a 0.02 mm spacing from the sides and adjacent panels. The rigid panels are considered to have the magnetic dipole moment of a neodymium n52 magnet of equal volume. The material of the silicone frame is chosen to be COMSOL's standard PDMS material, that has a Young's modulus of 750 kPa and a Poisson's ratio of 0.49.

The amount of magnetic torque applied on each side panel was calculated using Formula 2. A probe was used to calculate and update the angle between the magnetic field and the orientation of the panel's magnetic dipole moments. We were able to run this model from 1 to 52 mT, with a relative tolerance of 0.001. At 52 mT the maximum horizontal displacement of the panels was observed to be 0.18 mm, as seen in Figure 16. At this point, the capsule has a R-value of 1.85. This is 84% of this capsule's maximum R-value of 2.2.

Plotting the height and width of the capsule for different magnetic field values gives us Figure 17. In the figure it can be seen that the deformation rate starts to decrease as the magnetic field value increases. The

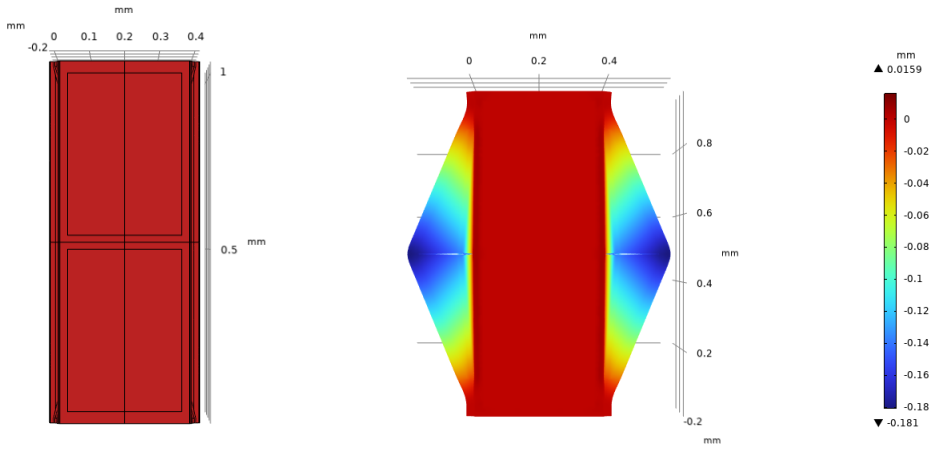

Figure 16: Deformation of the magnetic capsule in x-direction at magnetic field strength 0 mT (left) and 52 mT (right).

same observation is made when we look at the change in the angle of the side panels with the vertical axis, see Figure 18. These graphs indicate that the required magnetic field strength for deformation increases non-linearly. The angle between the magnetic field and the dipole moment at 52 mT is 70 degrees, which means that the magnetic torque is still 94% of the original value. Therefore, the decrease in deformation rate is not caused by a decline in magnetic torque. It must be the material that increasingly resists deformation. Unfortunately, the model could not be run past 52 mT, even if the mesh density was increased at places with high deformation gradients. An inspection of the geometry showed, that around 52 mT an overlap developed between the mesh areas of the outward folding triangles. This could potentially be the reason the model breaks at this magnetic field value.

Based on the trends seen in Figures 17 & 18, it is assumed that the force required to completely unfold the capsule is substantially larger than 52 mT. We desire to keep the required field strength under 100 mT to avoid the effects of magnetic saturation and to limit energy consumption. It is, therefore, necessary to improve the model so that the required field strength can be determined. If this value does indeed exceed 100 mT, alternations to the capsule design might be needed.

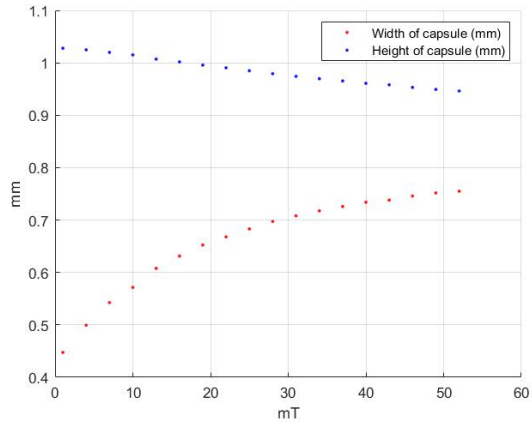

Figure 17: Width and height of origami capsule at different magnetic field strengths.

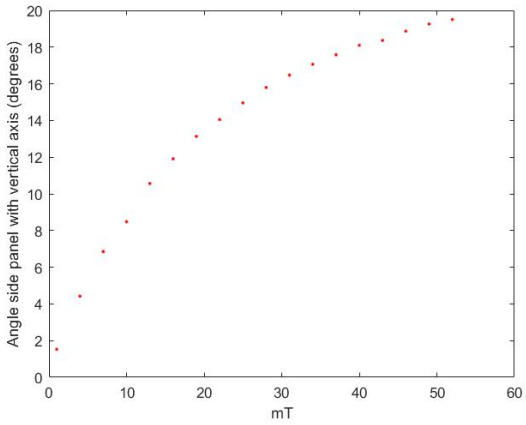

Figure 18: Angle of side panels with vertical axis at different magnetic field strengths.

6 Prototype

6.1 Prototype description

The prototype is an up-scaled version of the concept. It consists of multiple 1 mm thick PLA plates arranged within a silicone sheet. The sizes of these plates are shown in Figure 19. As stated in Section 4.3, the silicone sheet provides the elastic properties needed for flexible folding points between the plates. These folding points are created by spacing the plates 2 mm apart from one another within the silicone. The plates contain multiple holes (d= 2mm), that provide extra connection points between the silicone layers on both sides. This further strengthens the anchoring of the plates in the silicone. Silicone layers of 0.5 mm were successfully applied in the prototype, making the total thickness of the sheet approximately 2 mm. The silicone used for the prototype was Ecoflex 00-20 from Smooth-On. Ecoflex 00-20 is a platinum catalysed silicone, that consists of a part A and B. The silicone hardens after parts A and B are combined. This type of silicone can safely be exposed to the skin but is not certified for biomedical applications [36].

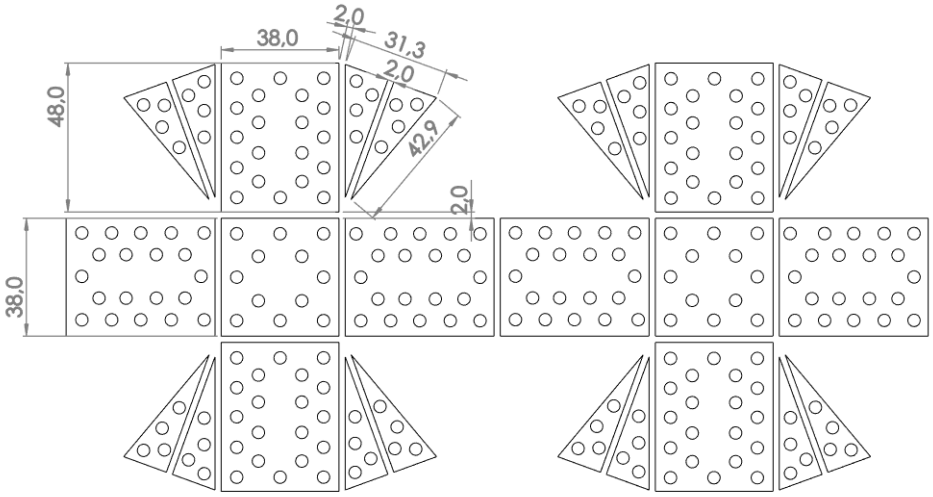

Figure 19: Plate sizes used in the prototype. Measurements are in mm.

The flat origami sheet must be connected to itself in order to get the unfolded capsule shape. This was done by applying a silicone adhesive to the sides and curing it while the plates were connected. The spacing between these connected plates must be approximately 2 mm, which requires the outer ends of the plates to be covered in 1 mm thick silicone. After the plates had been properly connected, we were left with the unfolded capsule shape. The plate sizes, shown in Figure 19, gave the unfolded structure an R-value of 2.2, with a width and height of 8.8 cm in the unfolded state. The folded capsule has a width of 4 cm and a height of 10 cm.

6.2 Fabrication

The PLA panels were 3D printed using the UltiMaker 2+ following the blueprint shown in Figure 19. To apply the silicone layers onto these panels, they are placed within an acrylic mold. This acrylic mold, shown in Figure 20, consists of a bottom plate and a plate with a cut out of the panel configuration. This cut out has an offset of +1 mm, so that the poured silicone forms 1 mm edges on the panel sides to which they can be attached to one another. The acrylic plates are firmly connected with bolts and nuts to prohibit silicone leakage.

Ecoflex 00-20 is prepared by mixing parts A and B in a 1:1 ratio. After properly mixing these parts, the air trapped in the silicone needs to be removed. For this reason, the silicone is put into a vacuum chamber

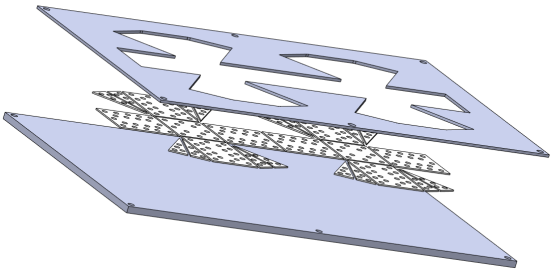

Figure 20: Manufacturing method of the prototype capsule. The origami panels are placed within an acrylic mold, which makes silicone application possible.

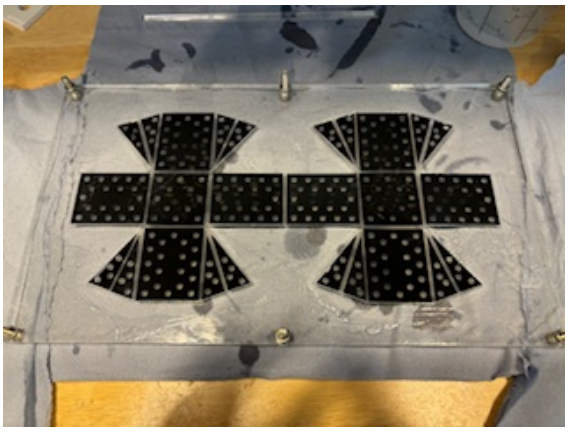

Figure 21: Image of the PLA panels covered in silicone, during the molding phase.

till no air is left escaping the liquid. The silicone can only be applied on one side at a time, which means that the process needs to be repeated after the first layer has hardened. If magnets were to be incorporated into the origami structure it had to be done during this stage of fabrication, so that they were enveloped in the silicone. The process left us with the flat origami sheet, as shown in Figure 21. The final stage of the fabrication is connecting the origami structure to itself using fast-hardening silicone adhesive. This step gave the product shown in Figure 22.

6.3 Results

Figure 22 shows the disconnected halves of the prototype foldable capsule. The prototype was produced in the unfolded state, which is due to the elastic nature of silicone the shape it returns to after the capsule is deformed. For this reason, it was not possible to test the magnetic unfolding capabilities of the prototype, as the elastic force would already unfold the capsule. This elastic force seemed to increase exponentially as the capsule was deformed manually. This is similar to the prediction made with the model in Section 5.3, where the resistance to deformation increased non-linearly.

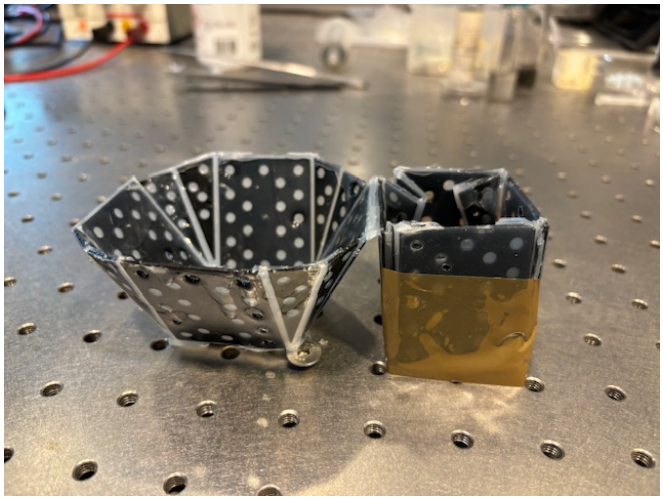

Figure 22: Bottom and top half of the prototype foldable capsule. The capsule halves are shown folded (right) and unfolded (left).

As it was not possible to test the magnetic unfolding of the prototype, it was decided to make a paper version. This paper version was used to visualise the workings of the concept. It was chosen to make only the bottom part of the capsule, as the weight of the added magnets would otherwise cause the complete capsule to unfold itself. The results of this experiment are shown in Figure 23. By switching the orientation of the magnet, the inward magnetic torques were turned into outward magnetic torques. These outward magnetic torques caused the capsule to unfold.

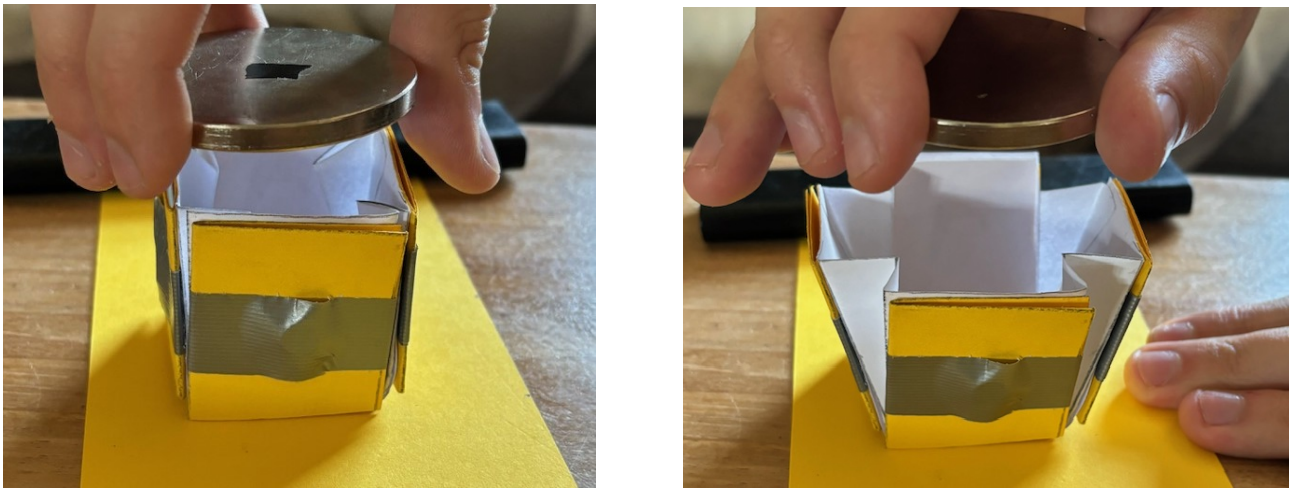

Figure 23: Magnetic unfolding of the bottom half of a paper capsule. In the left image, the magnet is orientated to cause an inward magnetic torque. In the right image, the magnet orientation is flipped to get an outward magnetic torque. The outward torque causes the capsule to unfold.

7 Discussion

7.1 Capsules applicability

Based on the results of the concept analysis and the prototype, there are multiple improvements that can be made to the design. These improvements should increase the effectiveness of magnetic locomotion and magnetic unfolding. Unfortunately, it is expected that increasing the range of usable R-values is not possible, as these are a direct consequence of the chosen design. For this reason, the improved design can only be used to treat aneurysms, which have a dome width of 1.24 times the width of the smallest blood vessel the capsule passes through. This value is based on a max R-value of 3.1 and a capsule-to-vessel ratio of 0.4. In the circle of Willis, the maximum vessel width is circa 5 mm [16]. This means that the maximum size aneurysm the capsule can treat is 6.2 mm, assuming the capsule does not travel through smaller vessels. Intracranial aneurysms with dome sizes of 5 mm - 10 mm fall in the medium category for the chance of rupture [17]. Therefore, in the most optimal scenario, the capsule could be used to treat aneurysms of the medium category. The used max R-value can however, only be used under the assumption that the capsule does not pass blood vessels with an angle greater than 70 degrees. This would otherwise decrease the achievable R-value below 3.1, as can be seen in Figure 13. For these reasons, the capsule's applications are limited.

7.2 Improving magnetic transportation

As discussed in Section 5.2, the expected maximum magnetic gradient necessary to transport the capsule to the aneurysm site might be larger than modern coiling systems can generate. The value of 85.7 T/m is however, based on the assumption that the blood velocity and viscosity have the highest values in their considered ranges, but the actual values may be lower. For this reason, the model must be validated with

experimental data to confirm that the chosen values are realistic. If these values are found to be good representations of the in vivo situation, two actions can be taken to decrease the necessary magnetic field gradient. The first option is to improve the fluid dynamics of the capsule by making the top and bottom more sphere-like. Spherical surfaces are more streamlined than flat ones, causing them to disturb the flow of liquid less. This effect is observed in the simulation if the cuboid capsule is changed for a spherical one, with the same diameter. The other option would be to increase the magnetic volume of the magnets, with dipole moments along the vertical axis. The inside of the capsule is mostly empty and can therefore be used to add more magnetic material. Increasing the total volume of these magnets by 4.4 times would bring the value for the needed magnetic gradient to the considered achievable range. Of these two options the first one is preferred, as it adds less weight to the capsule.

7.3 Improving magnetic unfolding

Based on the results of the model in Section 5.3, the needed magnetic strength to completely unfold the capsule, could exceed the chosen limit of 100 mT. This prediction is made by extrapolating the acquired data of the model until its breaking point. For this reason, the model needs to be improved so that the actual value can be determined. If this value does exceed the set limit, alterations need to be made to reduce the necessary magnetic field strength. Possible alterations are: increasing the magnetic volume of the magnets, using thinner layers of PDMS, and using an even softer connective material. These options will either decrease the amount of torque needed for deformation or increase the amount of torque generated by the same magnetic field. Another option would be to combine the usage of magnetic torque with a SMP. As discussed in Section 2.4, a capsule made out of an SMP will be able to retrieve its original shape after getting heated passed its transition temperature. With this method, the origami capsule can be made as a flat sheet and be connected to itself to form the unfolded capsule. This capsule can be shaped to its folded form and transported to the aneurysm site. With an alternating magnetic field the capsule can be heated, causing it to retrieve its unfolded shape inside the aneurysm dome [21]. This method would also resolve the problem of the prototype reverting to its folded state. It is, however, not possible to generate a homogeneous magnetic field and an alternating magnetic field, at the same time. Therefore, it is considered to use them consecutively. Magnetic torque is most efficient when the angle between the magnetic dipole moment and the external field is large, as discussed in Section 2.3. As this angle decreases the homogeneous field can be changed to an alternating one to finish the deformation with the properties of the SMP. This would reduce the maximum magnetic field strength needed. For this technique to work a SMP is required with a similar Young's modulus as silicone.

7.4 Alternative to simple coiling

This capsule was designed to be an alternative to the common method of aneurysm coiling. The main improvement of the design is that it does not have the drawbacks of coil compaction, coil migration, and incomplete aneurysm filling, which can occur after simple coiling [9]. Unfortunately, the origami capsule lacks the broad range of aneurysm sizes that can be treated with simple coiling. Therefore, the capsule is only considered to be an improvement for aneurysms of the sizes mentioned in Section 7.1. Aneurysms at these sizes do often not have a high chance of rupture [17]. For this reason, the design should be seen as a preventive option. It is minimally invasive and can be used to plug aneurysms before they increase in size and become a threat to the patient's health. This is without resorting to intracranial catheters, which makes it even less invasive than simple coiling.

8 Conclusion & Future work

The concept origami-based, magnetic capsule could be an improvement on the simple coiling technique for a small range of intracranial aneurysm sizes. Within this range, it offers a more stable filling material, than the platinum coils used in simple coiling. The aneurysms that can be treated using these techniques are small and have a low chance of rupture. Therefore, the capsule must be considered as a preventive treatment, which plugs smaller aneurysms before they grow and become a health risk.

The transportation and unfolding of the capsule will be achieved by the usage of magnetic force and torque. Simulations were performed to predict if the required magnetic field strength and gradient had reasonable values. The required magnetic gradient was found to be higher than achievable with systems specifically made for magnetic actuation. Two alterations to the design were proposed that could lower the required gradient to be in the workable range. Unfortunately, it was not possible to run the model for magnetic actuation to the point where the capsule was fully unfolded. Based on the available data it was assumed, that the needed magnetic field strength would be higher than preferred value of 100 mT. For this reason, more design alternations were considered to lower the required magnetic field strength. The most promising option is the combination of magnetic actuation with a SMP material.

In future research it is recommended to improve the model for magnetic actuation so that the actual required magnetic field strength can be determined. Furthermore, both models need to be validated with experimental data to confirm that their outputs have realistic values. If this is the case, the next step would be to make and test a true-size capsule, within a simulated environment. This would require redefining the fabrication process so that it can be used to create capsules within the millimetre range.

Disclaimer:

During the preparation of this work the author(s) used no artificial intelligence tools.

References

[1] J.-Y. Lee, B. B. Kang, D.-Y. Lee, S.-M. Baek, W.-B. Kim, W.-Y. Choi, J.-R. Song, H.-J. Joo, D. Park, and K.-J. Cho, "Development of a multi-functional soft robot (snumax) and performance in robosoft grand challenge," *Frontiers in Robotics and AI*, vol. 3, 2016.

[2] J. Novitzke, "The basics of brain aneurysms: a guide for patients," *J Vasc Interv Neurol*, vol. 1, no. 3, pp. 89–90, 2008.

[3] V. S. Alg, R. Sofat, H. Houlden, and D. J. Werring, "Genetic risk factors for intracranial aneurysms: a meta-analysis in more than 116,000 individuals," *Neurology*, vol. 80, no. 23, pp. 2154–65, 2013.

[4] N. Shaikh, A. Chanda, S. Nawaz, A. Alkubaisi, A. Alyafei, A. E. A. Ganaw, and M. F. Malmstrom, *Aneurysmal Subarachnoid Haemorrhage: Epidemiology, Aetiology, and Pathophysiology*, pp. 1–11. Cham: Springer International Publishing, 2022.

[5] J. Zhao, H. Lin, R. Summers, M. Yang, B. G. Cousins, and J. Tsui, "Current treatment strategies for intracranial aneurysms: An overview," *Angiology*, vol. 69, no. 1, pp. 17–30, 2018.

[6] W. Brinjikji, H. J. Cloft, and D. F. Kallmes, "Difficult aneurysms for endovascular treatment: overwide or undertall?," *AJNR Am J Neuroradiol*, vol. 30, no. 8, pp. 1513–7, 2009.

[7] The Medical Advisory Secretariat, "Coil embolization for intracranial aneurysms: an evidence-based analysis," *Ont Health Technol Assess Ser*, vol. 6, no. 1, pp. 1–114, 2006.

[8] W. Yue, "Endovascular treatment of unruptured intracranial aneurysms," *Interv Neuroradiol*, vol. 17, no. 4, pp. 420–4, 2011.

[9] H. Henkes, S. Fischer, T. Liebig, W. Weber, J. Reinartz, E. Miloslavski, and D. Kühne, "Repeated endovascular coil occlusion in 350 of 2759 intracranial aneurysms: safety and effectiveness aspects," *Neurosurgery*, vol. 58, no. 2, pp. 224–32; discussion 224–32, 2006.

[10] K. Kuribayashi, K. Tsuchiya, Z. You, D. Tomus, M. Umemoto, T. Ito, and M. Sasaki, "Self-deployable origami stent grafts as a biomedical application of ni-rich tini shape memory alloy foil," *Materials Science and Engineering: A*, vol. 419, no. 1, pp. 131–137, 2006.

[11] Q. Ze, S. Wu, J. Dai, S. Leanza, G. Ikeda, P. C. Yang, G. Iaccarino, and R. R. Zhao, "Spinning-enabled wireless amphibious origami millirobot," *Nature Communications*, vol. 13, no. 1, p. 3118, 2022.

[12] S. Miyashita, S. Guitron, M. Ludersdorfer, C. R. Sung, and D. Rus, "An untethered miniature origami robot that self-folds, walks, swims, and degrades," in *2015 IEEE International Conference on Robotics and Automation (ICRA)*, pp. 1490–1496, 2015.

[13] T. Xu, J. Zhang, M. Salehizadeh, O. Onaizah, and E. Diller, "Millimeter-scale flexible robots with programmable three-dimensional magnetization and motions," *Science Robotics*, vol. 4, no. 29, p. eaav4494, 2019.

[14] A. Keedy, "An overview of intracranial aneurysms," *Mcgill J Med*, vol. 9, no. 2, pp. 141–6, 2006.

[15] L. Hacein-Bey, T. C. Origitano, and J. Biller, "Chapter 15 - subarachnoid hemorrhage in young adults," in *Stroke in Children and Young Adults (Second Edition)* (J. Biller, ed.), pp. 289–314, Philadelphia: W.B. Saunders, second edition ed., 2009.

[16] S. Kamath, "Observations on the length and diameter of vessels forming the circle of willis," *J Anat*, vol. 133, no. Pt 3, pp. 419–23, 1981.

[17] W. C. Merritt, H. F. Berns, A. F. Ducruet, and T. A. Becker, "Definitions of intracranial aneurysm size and morphology: A call for standardization," *Surg Neurol Int*, vol. 12, p. 506, 2021.

[18] N. Ebrahimi, C. Bi, D. Cappelleri, G. Ciuti, A. Conn, D. Faivre, N. Habibi, A. Hošovský, V. Iacovacci, I. Khalil, V. Magdanz, S. Misra, C. Pawashe, R. Rashidifar, P. Soto-Rodriguez, Z. Fekete, and A. Jafari, "Magnetic actuation methods in bio/soft robotics," *Advanced functional materials*, vol. 31, Mar. 2021.

[19] W. Chen, J. Sui, and C. Wang, "Magnetically actuated capsule robots: A review," *IEEE Access*, vol. 10, pp. 88398–88420, 2022.

[20] T. Xu, J. Zhang, M. Salehizadeh, O. Onaizah, and E. Diller, "Millimeter-scale flexible robots with programmable three-dimensional magnetization and motions," *Science Robotics*, vol. 4, no. 29, p. eaav4494, 2019.

[21] M. Behl and A. Lendlein, "Shape-memory polymers," *Materials Today*, vol. 10, no. 4, pp. 20–28, 2007.

[22] R. L. Dodd and G. K. Steinberg, "Aneurysms," in *Encyclopedia of the Neurological Sciences* (M. J. Aminoff and R. B. Daroff, eds.), pp. 161–172, New York: Academic Press, 2003.

[23] D. da Silva, M. Kaduri, M. Poley, O. Adir, N. Krinsky, J. Shainsky-Roitman, and A. Schroeder, "Biocompatibility, biodegradation and excretion of polylactic acid (pla) in medical implants and theranostic systems," *Chem Eng J*, vol. 340, pp. 9–14, 2018.

[24] M. Zare, E. Rezvani Ghomi, P. Venkatraman, and S. Ramakrishna, "Silicone-based biomaterials for biomedical applications: Antimicrobial strategies and 3d printing technologies," *Journal of Applied Polymer Science*, vol. 138, 05 2021.

[25] D. D. München and H. M. Veit, "Neodymium as the main feature of permanent magnets from hard disk drives (hdds)," *Waste Management*, vol. 61, pp. 372–376, 2017.

[26] V. Iacovacci, I. Naselli, A. R. Salgarella, F. Clemente, L. Ricotti, and C. Cipriani, "Stability and in vivo safety of gold, titanium nitride and parylene c coatings on ndfeb magnets implanted in muscles towards a new generation of myokinetic prosthetic limbs," *RSC Advances*, vol. 11, no. 12, pp. 6766–6775, 2021.

[27] A. Sidiq, R. J. Gravina, S. Setunge, and F. Giustozzi, "High-efficiency techniques and micro-structural parameters to evaluate concrete self-healing using x-ray tomography and mercury intrusion porosimetry: A review," *Construction and Building Materials*, vol. 252, p. 119030, 2020.

[28] L. Leal Filho, T. Souza, O. Lima, and F. Leal, "Sphericity of apatite particles determined by gas permeability through packed beds," *Minerals and Metallurgical Processing*, vol. 26, p. 105, 05 2009.

[29] R. Sharp, P. Carr, J. Childs, A. Scullion, M. Young, T. Flynn, C. Kirker, G. Jackson, and A. Esterman, "Catheter to vein ratio and risk of peripherally inserted central catheter (picc)-associated thrombosis according to diagnostic group: a retrospective cohort study," *BMJ Open*, vol. 11, no. 7, p. e045895, 2021.

[30] E. Nader, S. Skinner, M. Romana, R. Fort, N. Lemonne, N. Guillot, A. Gauthier, S. Antoine-Jonville, C. Renoux, M. D. Hardy-Dessources, E. Stauffer, P. Joly, Y. Bertrand, and P. Connes, "Blood rheology: Key parameters, impact on blood flow, role in sickle cell disease and effects of exercise," *Front Physiol*, vol. 10, p. 1329, 2019.

[31] E. Doutel, F. Galindo-Rosales, and L. Campo-Deaño, "Hemodynamics challenges for the navigation of medical microbots for the treatment of cvds," *Materials*, vol. 14, p. 7402, 12 2021.

[32] D. Neugebauer, Y. Zhang, T. Pakula, S. S. Sheiko, and K. Matyjaszewski, "Densely-grafted and double-grafted peo brushes via atrp. a route to soft elastomers," *Macromolecules*, vol. 36, no. 18, pp. 6746–6755, 2003. doi: 10.1021/ma0345347.

[33] J. Orellana Barrasa, A. Ferrández-Montero, B. Ferrari, and J. Y. Pastor, "Characterisation and modelling of pla filaments and evolution with time," *Polymers (Basel)*, vol. 13, no. 17, 2021.

[34] D. Rao and M. Bagianathan, "Selection of optimal magnets for traction motors to prevent demagnetization," *Machines*, vol. 9, p. 124, 06 2021.

[35] D. Li, F. Niu, J. Li, X. Li, and D. Sun, "Gradient-enhanced electromagnetic actuation system with a new core shape design for microrobot manipulation," *IEEE Transactions on Industrial Electronics*, vol. 67, no. 6, pp. 4700–4710, 2020.

[36] Smooth-On, Inc., "Ecoflex™ 00-20 product information." `https://www.smooth-on.com/products/ecoflex-00-20/`. Accessed: 8-7-2024.

A Appendix

A.1 Design A

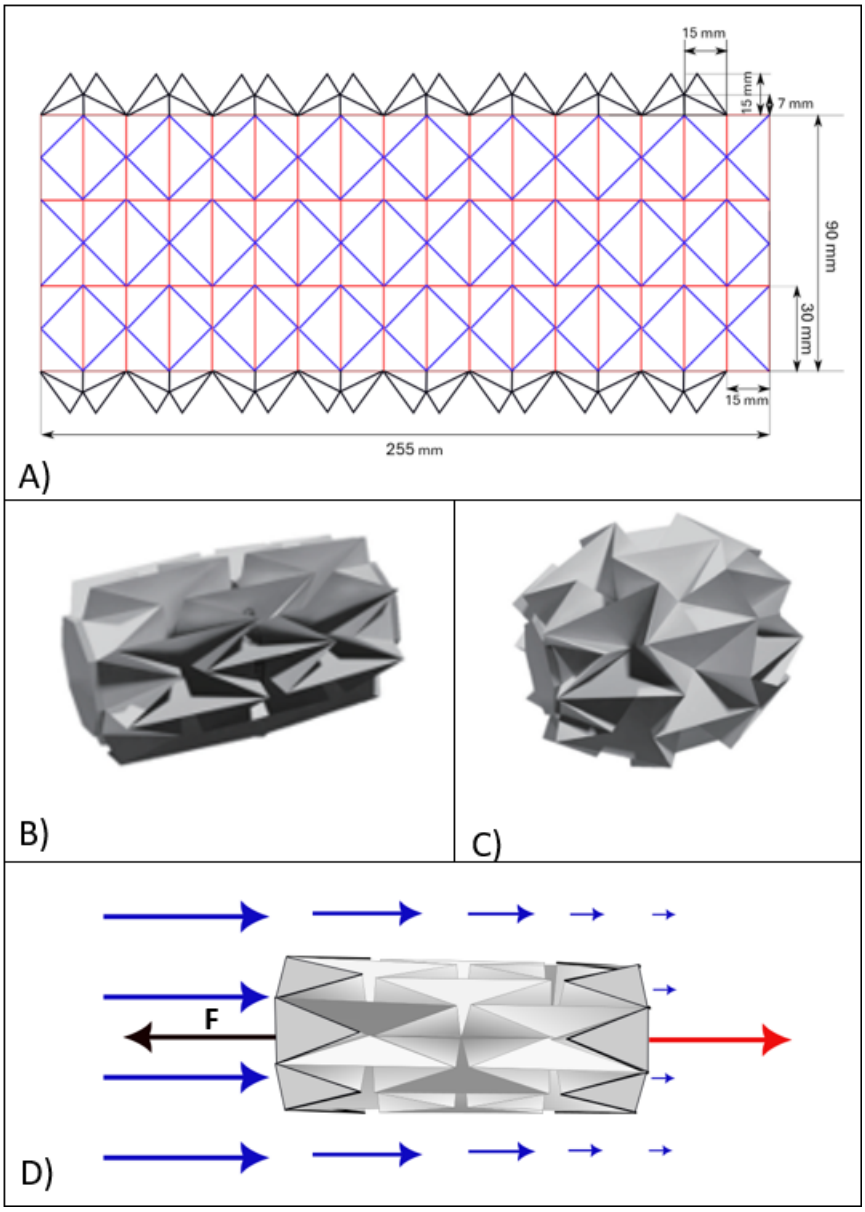

Figure 24: A) Layout of an expanding origami capsule based on the waterbomb pattern with dimensions. The pattern is repeated 3x8 times and has a region of overlap on the right side. An extra pattern has been applied to the top and bottom, that forms two octagonal caps at each end. B) Folded capsule shape [1]. C) Unfolded capsule shape [1]. D) Method of magnetic actuation. The capsule is pulled towards the increasing magnetic gradient (blue arrows) by a magnetic force (black arrow). The magnetic dipole moments (red arrows) are aligned with the external field.

A.2 Design B

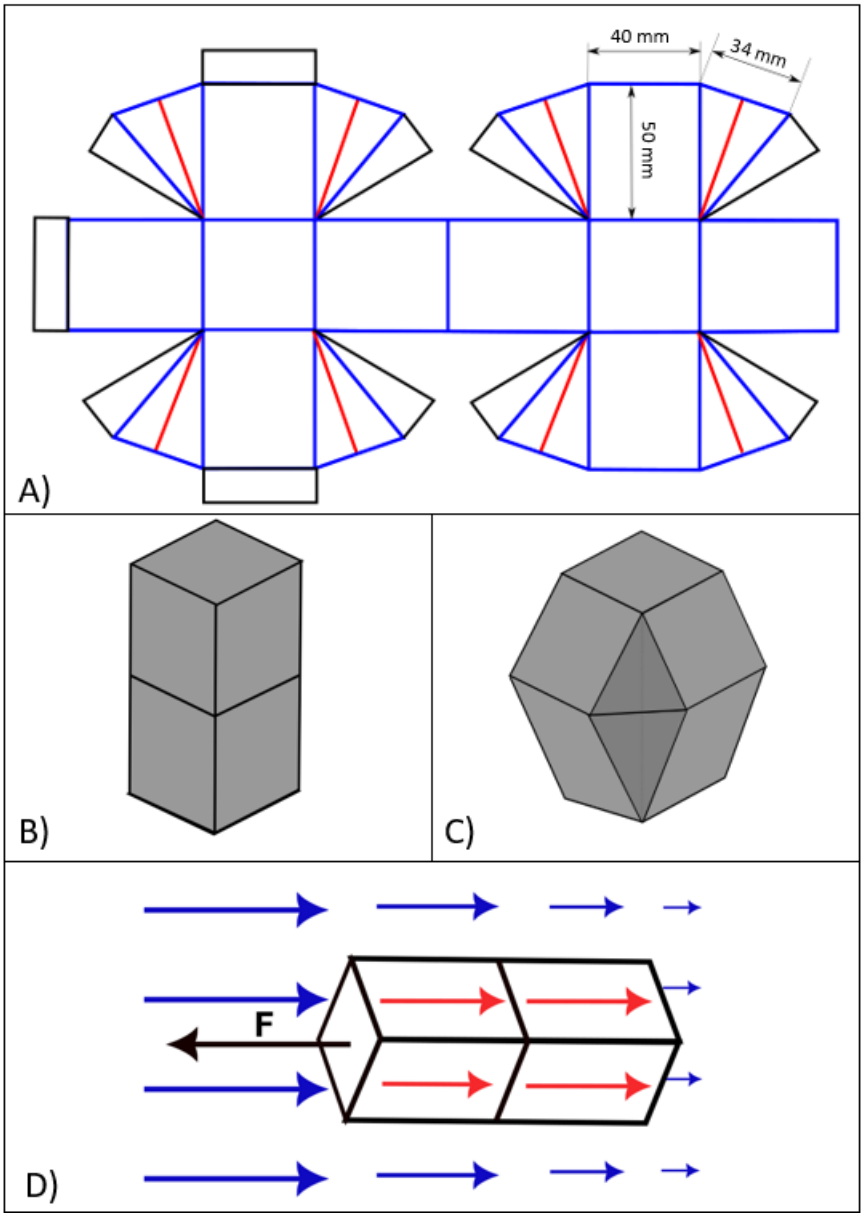

Figure 25: A) Layout of the cuboid shaped origami capsule with dimensions. The black coloured shapes are connecting pieces. B) Capsule in the folded state. C) Capsule in the unfolded state. D) Method of magnetic actuation. The capsule is pulled towards the increasing magnetic gradient (blue arrows) by a magnetic force (black arrow). The magnetic dipole moments (red arrows) are aligned with the external field.

A.3 Design C

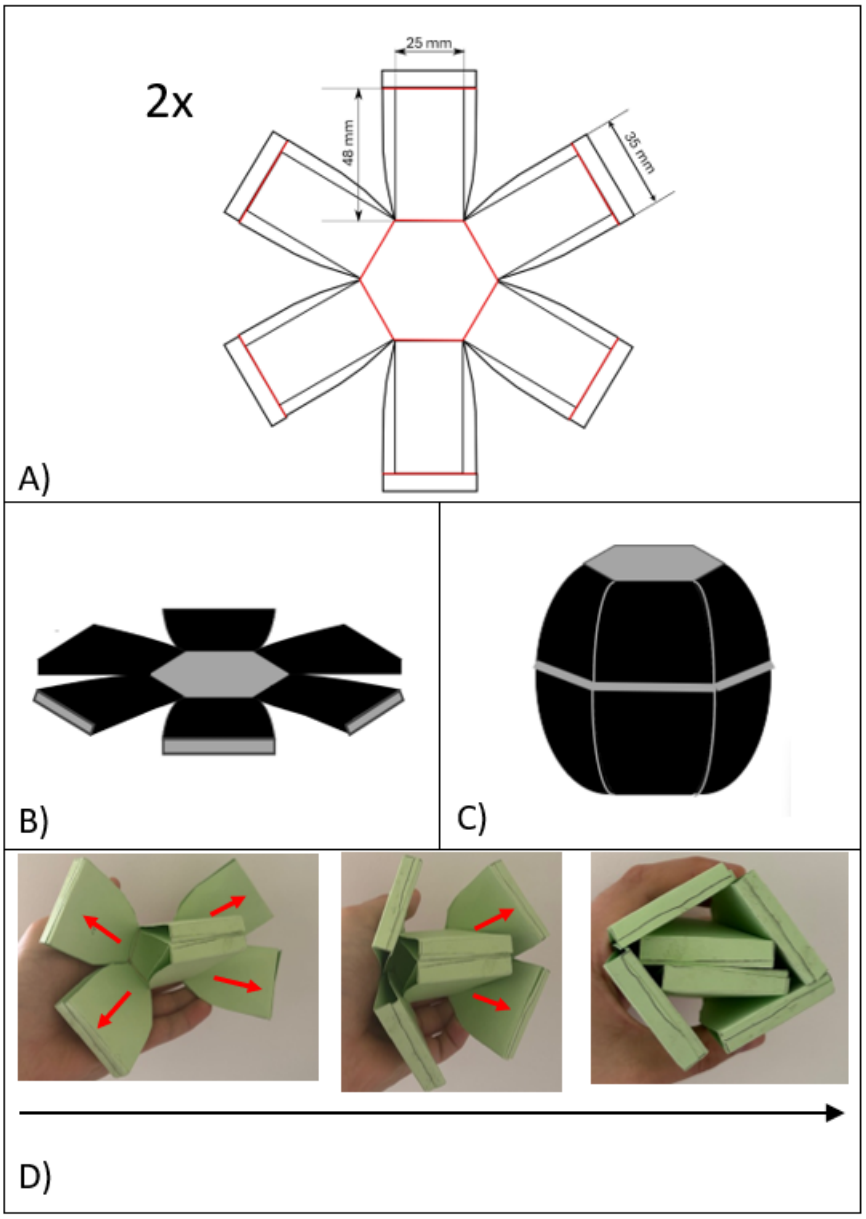

Figure 26: A) Layout of compressible origami sphere with dimensions. Two of these asterisk shaped sheets are connected to each other at the end of each arm at the red fold lines. In order to get the spherical shape once unfolded, the arms are slightly bent towards the centre at the sides. B) Flattened origami sphere. C) Expended origami sphere. D) Method of magnetic actuation. Two of the arms are folded inwards while the other four act as flippers to propel the structure through a liquid. The motion of the flippers is caused by magnetic torques, that try to align the magnetic dipole moments (red arrows) with the external magnetic field that is opposite to the direction of motion. The order of flipper movement is shown in the direction of the black arrow.

A.4 Design D

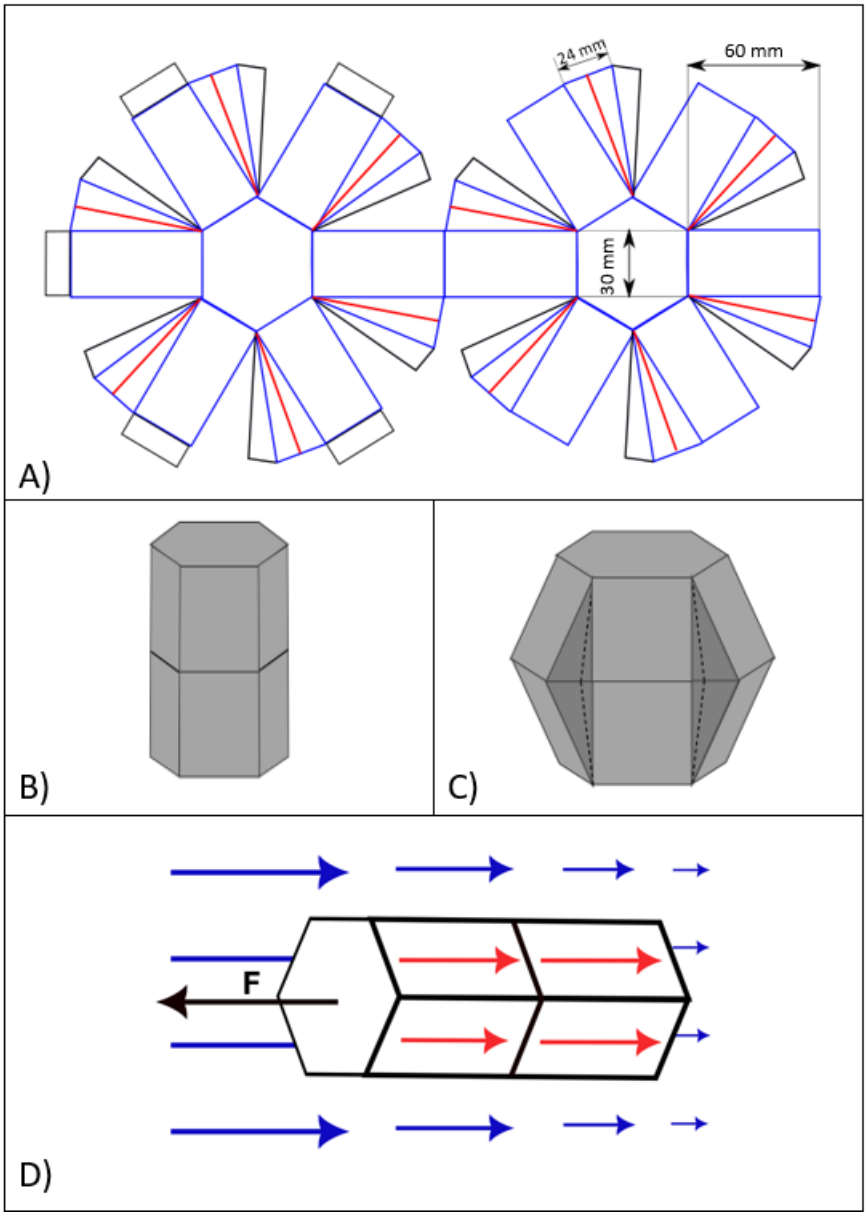

Figure 27: A) Layout of hexagonal prism shaped origami capsule with dimensions. The black coloured shapes are connecting pieces. B) Folded capsule shape. C) Unfolded capsule shape. D) Method of magnetic actuation. The capsule is pulled towards the increasing magnetic gradient (blue arrows) by a magnetic force (black arrow). The magnetic dipole moments (red arrows) are aligned with the external field.

A.5 Requirements & constraints

Requirements& Constraints	Grade 1	Grade 2	Grade 3	Grade 4	Grade 5	weight (1-3)
Magnetic transportation	The actuation of the capsule cannot be achieved with magnetic fields.	The actuation of the capsule requires a magnetic field, which directional vectors vary in between the -180 and 180 degrees within the workspace.	The actuation of the capsule requires a magnetic field, which directional vectors vary in between the -90 and 90 degrees within the workspace.	The actuation of the capsule requires a magnetic field, which directional vectors vary in between the -45 and 45 degrees within the workspace.	The actuation of the capsule requires an one directional (non -) homogeneous magnetic field.	1
Capsule flexibility	The end of the capsule bends < 20 degrees of the vertical axis.	The end of the capsule bends ≥ 20 degrees of the vertical axis.	The end of the capsule bends ≥ 30 degrees of the vertical axis.	The end of the capsule bends ≥ 40 degrees of the vertical axis.	The end of the capsule bends ≥ 50 degrees of the vertical axis.	1
Ease of production	The total amount of creases in the main origami body is > 300.	The total amount of creases in the main origami body is ≤ 300.	The total amount of creases in the main origami body is ≤ 200.	The total amount of creases in the main origami body is ≤ 100.	The total amount of creases in the main origami body is ≤ 50.	2
Unfolded-to-folded diameter ratio	The unfolded-to-folded diameter ratio is < 1.2	The unfolded-to-folded diameter ratio is ≥ 1.2	The unfolded-to-folded diameter ratio is ≥ 1.6	The unfolded-to-folded diameter ratio is ≥ 2	The unfolded-to-folded diameter ratio is ≥ 2.4	3
Strength in fold direction	The angle between the fold direction and the direction of compressive force is between 0° and 20°.	The angle between the fold direction and the direction of compressive force is between 20° and 40°.	The angle between the fold direction and the direction of compressive force is between 40° and 60°.	The angle between the fold direction and the direction of compressive force is between 60° and 80°.	The angle between the fold direction and the direction of compressive force is between 80° and 90°.	2
Shape unfolded state	The difference in volume between the unfolded capsule and that of a sphere with the same width is more than 40%, and/or the width-to-height ratio (R) is not 0.9 ≤ R ≤ 1.1.	The difference in volume between the unfolded capsule and that of a sphere with the same width is between 30-40%. Furthermore, the width-to-height ratio (R) is 0.9 ≤ R ≤ 1.1.	The difference in volume between the unfolded capsule and that of a sphere with the same width is between 20-30%. Furthermore, the width-to-height ratio (R) is 0.9 ≤ R ≤ 1.1.	The difference in volume between the unfolded capsule and that of a sphere with the same width is between 10-20%. Furthermore, the width-to-height ratio (R) is 0.9 ≤ R ≤ 1.1.	The difference in volume between the unfolded capsule and that of a sphere with the same width is between 0-10%. Furthermore, the width-to-height ratio (R) is 0.9 ≤ R ≤ 1.1.	2

Figure 28: Requirements & constraints based grading system for concept evaluation. The concepts are graded on a scale of 1 to 5 in each category. Based on the importance of the category an extra weight is assigned (1-3), that increases the fraction of points that its worth.

A.6 Evaluation of designs

Table 1: Point evaluation design A

requirements & constraints	**Score**	**Weight**	**Adjusted score**	**Note**
Magnetic transportation	5	1	5	
Capsule flexibility	2	1	2	Bending of circa 20 degrees observed in paper prototype.
Ease of production	2	2	4	
Unfolded-to-folded diameter ratio	4	3	12	Observed in paper prototype.
Strength in fold direction	5	2	10	
Shape unfolded state	5	2	10	Volume of cavities neglected, because blood is trapped within and cannot flow.
total:			**43**	

Table 2: Point evaluation design B

requirements & constraints	**Score**	**Weight**	**Adjusted score**	**Note**
Magnetic transportation	5	1	5	
Capsule flexibility	1	1	1	Folded capsule is rigid.
Ease of production	5	2	10	
Unfolded-to-folded diameter ratio	4	3	12	
Strength in fold direction	5	2	10	
Shape unfolded state	4	2	8	
total:			**46**	

Table 3: Point evaluation design C

requirements & constraints	**Score**	**Weight**	**Adjusted score**	**Note**
Magnetic transportation	4	1	4	
Capsule flexibility	1	1	1	Once completely folded no flexibility left.
Ease of production	5	2	10	
Unfolded-to-folded diameter ratio	3	3	9	Observed in paper prototype.
Strength in fold direction	1	2	2	
Shape unfolded state	5	2	10	
total:			**36**	

Table 4: Point evaluation design D

requirements & constraints	**Score**	**Weight**	**Adjusted score**	**Note**
Magnetic transportation	5	1	5	
Capsule flexibility	1	1	1	Folded capsule is rigid.
Unfolded-to-folded diameter ratio	4	3	12	
Strength in fold direction	5	2	10	
Shape unfolded state	4	2	8	
total:			**44**	